03,11

Zonal structure of graphene-like 2D allotropes of silicon carbide

© D.A. Zhukalin, A.V. Tuchin, A.V. Kalashnikov, Ya.S. Chasovskikh, E.N. Bormontov, I.I. Dolgih

Voronezh State University,
Voronezh, Russia

E-mail: zhukalin@vsu.ru

Received November 5, 2024
Revised December 27, 2024
Accepted December 28, 2024

The study investigates the energy characteristics of low-dimensional structures based on monolayers of 2D silicon carbide (2D-SiC). From the entire variety of possible polytypic forms, a subclass of graphene-like structures with a number of layers from 1 to 4 is distinguished. As a result of the analysis of the obtained data, dependencies of the band gap width and the location of the zone boundaries on the type of packing were identified. It was established that in the studied range of the number of layers, with constant stoichiometry, the layer-by-layer growth of structures leads to a decrease in the band gap width, and a change in the mutual orientation of the layers in the structure leads to a shift of the extrema on the band diagram and the formation of both direct and indirect bandgap semiconductors. The results allowed us to substantiate the reasons for the observed patterns from a physical point of view. The discrete series of bandgap widths of the investigated subset of structures ranges from 0.82 to 2.15 eV, covering the spectrum from visible to the IR range. The change in the crystal lattice of the *ABAB* structure and the reduction of the bandgap width to near-zero is of interest.

Keywords: semiconductors, low-dimensional materials, silicon carbide, band structure, first-principles calculations.

DOI: 10.61011/PSS.2025.01.60585.294

1. Introduction

Dimension is one of the important characteristics of a material that determines its structure and functional properties. For example, the familiar graphite material, upon transition to a two-dimensional state, acquires unique electrophysical properties and opens up a whole field for theoretical and experimental research [1]. Currently, the features of two-dimensional and quasi-two-dimensional semiconductor materials such as graphene, silicene, boron and gallium nitrides, silicon, boron and aluminum carbides are actively studied [2–4]. The silicon carbide (SiC) is of particular interest in this series. Materials based on it demonstrate a set of unique electronic and optical properties that open up new possibilities for practical applications in advanced designs of nanodevices [5,6]. However, the main attention of other authors is focused on studying the various stoichiometric compositions of the silicon carbide monolayer and the effect of embedded impurities. Studies on the types of packaging of graphene-like silicon carbide monolayers are extremely rare. This creates a gap in understanding the dependence of the characteristics of multilayer structures on the type of packaging of monolayers.

The structure-dependent properties of a family of multilayer silicon carbide allotropes, differing in the number and mutual orientation of the layers, were previously studied using the ab initio methods of quantum chemistry [7,8]. As a result, the formation of a number of stable allotropic modifications with attractive electrophysical characteristics for the development of nanoelectronics devices was revealed. The purpose of this study is to determine the dependence of the band structure and electrophysical properties of low-dimensional SiC on the topology of the lattice cell with 1 to 4 layers.

2. Objects and methods of research

The object of the study is multilayer structures based on atomically thin silicon carbide, which are topological analogues of graphene with 1−4 layers. Each layer of such a structure is a graphene-like sublattice composed of sequentially alternating silicon and carbon atoms. The following configurations are considered (Figure 1, projection in the plane formed by the vectors of the crystal lattice, the structure is presented before the optimization process):

1. SiC monolayer structure (type *A*);
2. structures of type $A\bar{A}$, with inversion of atoms in even layers;
3. structures of *AB* type, obtained by shifting even layers relative to odd ones in such a way that carbon atoms are located in the centers of hexagonal cells of odd layers.

In addition to the types of structures described above, other possible packings were also considered in previous studies [7]: such as *AA*, obtained by superimposing monolayers without inversion of atoms or displacement of layers; such as $A\bar{B}$, obtained from *AB* by inversion of atoms in even layers; as well as intermediate variants obtained by shifting even layers to other distances. The results of modeling of these packages showed that the structures with the highest bond energy between the layers correspond to the type $A\bar{A}$ (and therefore they are the most stable). Metastable structures include packings *AA* and *AB*. The

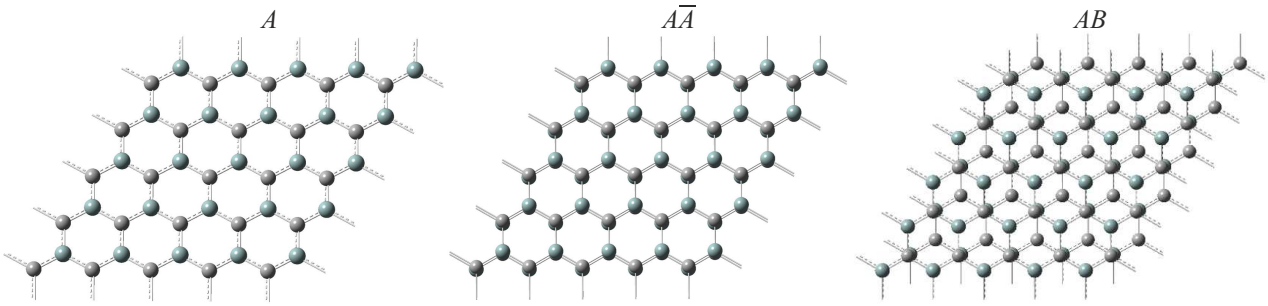

Figure 1. Fragments of the considered 2D allotropes of SiC before optimization of the structure.

remaining monolayer packings have become much less energetic, which indicates their instability, and therefore limits the possibility of their synthesis and application in device design. *AA* structures were not studied in detail in this paper due to the greater interest in *AB* type packing, which demonstrates a direct band gap and is therefore the most interesting for use in optical devices.

The calculations were performed using a specialized software system for solving quantum chemical problems Gaussian 9. The calculations were performed using the density functional theory (DFT) method in the local spin density approximation (LSDA) using the valence-split basis 3-21G. Periodic boundary conditions of a two-dimensional crystal lattice were used. The number of points in k-space is 80 000. The choice of the LSDA approximation is based on data from a number of theoretical studies on the properties of similar two-dimensional materials (graphene, silicene, various SiC isomers) [9–12]. The correctness of the chosen method was confirmed by modeling a single-layer silicon carbide using various bases and approximations available in the Gaussian package. The similarity of the values of the bond length ($R_{\mathrm{Si-C}}$) and the reduced bond energy (E_b) of the structure with experimental and theoretical data from literary sources was chosen as the criterion of correctness. The LSDA approximation in the 3-21G basis gives the results closest to the data from other studies according to the obtained results. For instance, the values of bond length ($R_{\mathrm{Si-C}} = 1.805$ Å) and bond energy ($E_b \sim 8.3$ eV/atom) obtained by us are confirmed by previous studies [13–17]. At the same time, the band gap of the monolayer E_g turned out to be equal to 2 eV, which is on average 0.5 eV less than in other studies. Considering that the width of the band gap of materials is less than the actual values in the LSDA approximation [18], the values of the width of the band gaps should actually be higher by ~ 0.5 eV. Thus, the results of the work are qualitative in nature, allowing us to see the patterns that arise when changing the parameters of structures. This may also be useful when considering, for example, the optical properties of multilayer silicon carbide. The calculation of the remaining structures was carried out under the assumption that, due to the identity of the research methods and structural parameters (lattice cell of the monolayer, stoichiometry), the level of confidence in the results remains the same as in the data for a single-layer structure.

The electrophysical characteristics of the considered family of structures were obtained in two stages. At the first stage, the geometry of the initial structures was optimized to minimize the potential energy surface. At the second stage, the band structures were calculated for the optimal configurations obtained.

A graphene lattice cell was used as the basic lattice cell for the optimization process, in which one of the carbon atoms was replaced by a silicon atom. A geometric configuration corresponding to a lattice in which the charge density balance condition is met (the total charge is zero) was obtained based on the modeling results. The parameters of the initial geometry of the monolayer (permanent lattices, interatomic bonds, and the position of atoms relative to the translation vectors while maintaining the hexagonal structure) varied within different limits for confirming the stability of the obtained solution. Repeated modeling of the modified structures showed that all the initial topological configurations lead to the same solution, thereby confirming stability.

The main energy characteristics of 2D allotropes of SiC were calculated based on the data obtained. Since a limited number of points in k-space were used to construct the band diagrams, the intermediate values in the diagram were obtained as a result of interpolation. The calculation results are listed in the table. All calculations were obtained in the Supercomputing Center of Voronezh State University.

The reduced bond energy was calculated using the formula:

$$E_b = \frac{NE_{\mathrm{tot}}(\mathrm{Si}) + NE_{\mathrm{tot}}(\mathrm{C}) - E_{\mathrm{tot}}(\mathrm{Si}_N\mathrm{C}_N)}{2N},$$

where $E_{\mathrm{tot}}(\mathrm{Si})$, $E_{\mathrm{tot}}(\mathrm{C})$, $E_{\mathrm{tot}}(\mathrm{Si}_N\mathrm{C}_N)$ is the total energy of a solitary silicon atom, carbon, and a structure containing N silicon atoms and N carbon atoms.

The reduced interplanar bond energy was calculated using the formula:

$$E_{bsh} = \frac{nE_{\mathrm{tot}}(\mathrm{SiC}) - E_{\mathrm{tot}}(\mathrm{Si}_N\mathrm{C}_N)}{n},$$

where $E_{\mathrm{tot}}(\mathrm{SiC})$, $E_{\mathrm{tot}}(\mathrm{Si}_N\mathrm{C}_N)$ is the total energy of a single-layer silicon carbide and n-layered structure containing

N silicon atoms and N carbon atoms. Electrophysical properties of 2D silicon carbide allotropes depending on the number and configuration of layers ($R_{\mathrm{Si-C}}$ is the bond length between carbon and silicon atoms within the layer; R_{sh} is the interlayer distance, E_b is the reduced bond energy; E_{bsh} is the reduced interplane bond energy; $E_{g(i)}$, $E'_{g(i)}$ is the band gap width in the directions $M\Gamma K$ and $M'\Gamma K'$; $E_{g(d)}$, $E'_{g(d)}$ is the width of the band gap at a straight-band transition in the directions $M\Gamma K$ and $M'\Gamma K'$).

3. Results and discussion

The basic structure for analyzing the evolution of electrophysical properties during layer-by-layer growth is a silicon carbide monolayer. The band diagram and the energy distributions of the orbitals are shown in Figure 2. The atoms formed a planar structure with hexagonal symmetry $\bar{6}m2$ after relaxation. The length of the chemical bond $R_{\mathrm{Si-C}} = 1.80$ Å, which is 0.38 Å longer than the bond length in graphene. The highest occupied and lowest free orbitals, as in the case of graphene, are formed by π- and π^*-bound p_z-orbitals of atoms of the crystal lattice [11]. Unlike graphene, silicon carbide is a semiconductor with the width of interband junction E_g of the order of 2 eV (see the table). A comparative analysis of the topologies, band structures, and energy characteristics of graphene and single-layer silicon carbide allows us to identify the following features characteristic of the latter: the presence of atoms with different electronegativity, increased bond length and lattice constant, and a higher density of electronic orbitals in a silicon atom. These features led to the elimination of the degeneration of energy levels at the point K and the formation of a band gap. The high symmetry of the lattice cell of the silicon carbide monolayer, similar to the graphene cell, leads to the localization of the maximum of the valence band and the minimum of the conduction band at one point of k-space, that is, the structure is a direct band gap semiconductor.

Let's consider structures of the type $A\bar{A}$, with inverted atoms on even layers. The three-layer structure retains the symmetry $\bar{6}m2$, while the two- and four-layer structures have changed the symmetry group to $\bar{3}m$. The inversion of atoms, or an identical shift operation, leads to the fact that an interlayer bond is formed due to the overlap of all $3p_z$-silicon orbitals and $2p_z$-carbon orbitals. The interlayer bond length is greater ($R_{sh} = 2.2$ Å) in these structures than the interatomic distance in the SiC-3C polytype in the state of hybridization sp^3 ($R_{\mathrm{Si-C-3C}} = 1.89$ Å) [19]. At the same time, the bond length within the layer slightly increased $R_{\mathrm{Si-C-}A\bar{A}}) = 1.864$ Å). The values of these values are in good agreement with the results of previous studies [20–22]. However, the authors showed in Ref. [20] that the atoms of the layers ceased to be in the same plane. This shows the predominance of the contribution of sp^3-hybridization to the interlayer bond. Our results show that the planarity of the layers has not been violated, that is, more preference is given to sp^2-hybridization. Such a discrepancy in the results is not unusual, since in such structures there is competition between the types of hybridization [23].

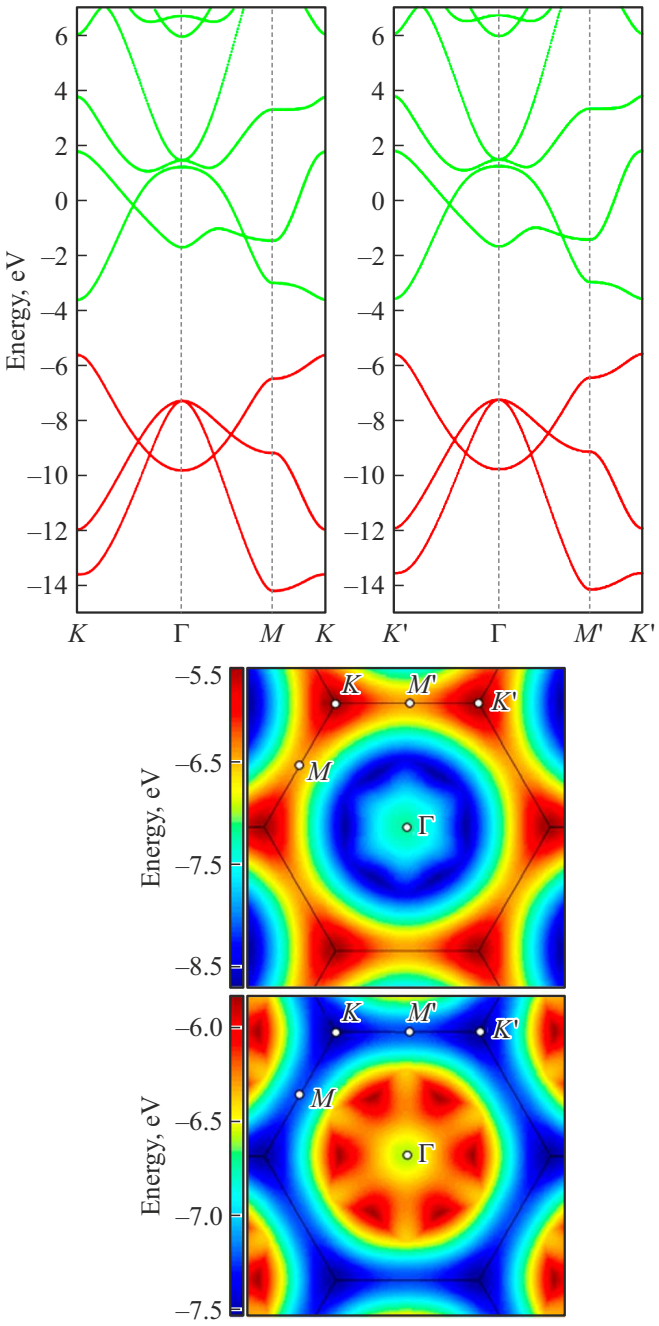

Figure 2. Band structure of the SiC monolayer (left), energy distribution of the highest occupied orbital (HO-orbital) (top right) and the lowest unoccupied orbital (LU-orbital) (bottom right).

The high bond energy of the layers ($E_{bsh-A\bar{A}} = 0.242$ eV/atom, $E_{bsh-A\bar{A}A} = 0.403$ eV/atom) (see table) shows that the layers have a strong impact on each other. The band diagrams have undergone significant changes (Figure 3). Due to the resulting partial σ-interaction, the highest occupied (HOMO) and lowest unoccupied

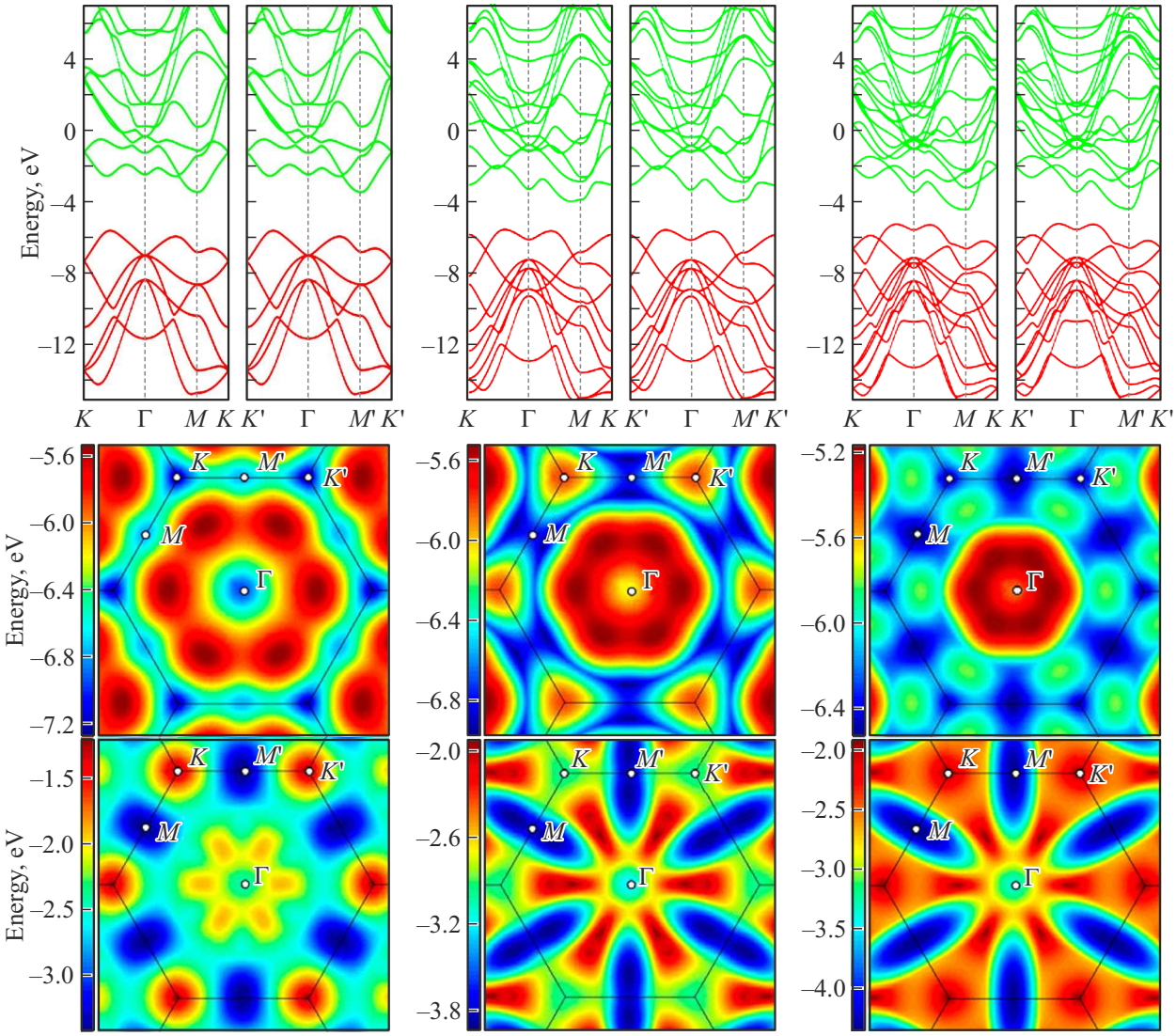

Figure 3. From left to right: data for structures $A\bar{A}$, $A\bar{A}A$ and $A\bar{A}A\bar{A}$. Upper row — band structures, middle row — energy distribution of the HO-orbital, lower row — energy distribution of the LU-orbital.

(LUMO) orbitals changed the location of the extremes. The diagram of the single-layer structure shows that the highest σ-bound orbitals have a maximum at Γ. Since there was a minimum in π-bound orbitals at this point, the combination of σ- and π-interactions shifts the ceiling of the valence band to the middle of the direction Γ$-K$, approaching the point Γ as the number of layers increases. By a similar mechanism, the bottom of the conduction band shifted from the position K to the position M. Thus, unlike a monolayer, the structures $A\bar{A}$ are indirect band gap semiconductors. An increase of the number of layers leads to an increase of the density of states, which in turn leads to a decrease of the width of the interband junction. The values for the two-, three-, and four-layer configurations E_g are 2.15, 1.57, and 0.82 eV, respectively, and the differences in directions ΓMK and Γ$M'K'$ do not exceed 0.01 eV (see table). The resulting dependence contrasts with the results of Ref. [24]. The authors demonstrated that the band gap does not depend on the number of layers and remains almost constant.

The opposite situation is observed in structures of the type AB (with offset lattices on even layers). The displacement of the layers led to the fact that only half of the carbon atoms of the even layers and silicon of the odd layers participate in the formation of the interlayer bond. The remaining atoms are located in the center of the hexagons formed by atoms of neighboring layers and indirectly participate in the formation of interlayer bonding. At the same time, the unhybridized orbitals began to have a smaller area of overlap between the layers. Therefore, the interlayer interaction in these structures is on average 1.6−1.8 times less than in structures of the type $A\bar{A}$ ($E_{bsh-A\bar{A}} = 0.242$ eV/atom and $E_{bsh-AB} = 0.156$ eV/atom). This results in an increase of the length of the interlayer bond ($E_{sh-A\bar{A}} = 2.2$ Å and $E_{sh-AB} = 3.243$ Å) (see the

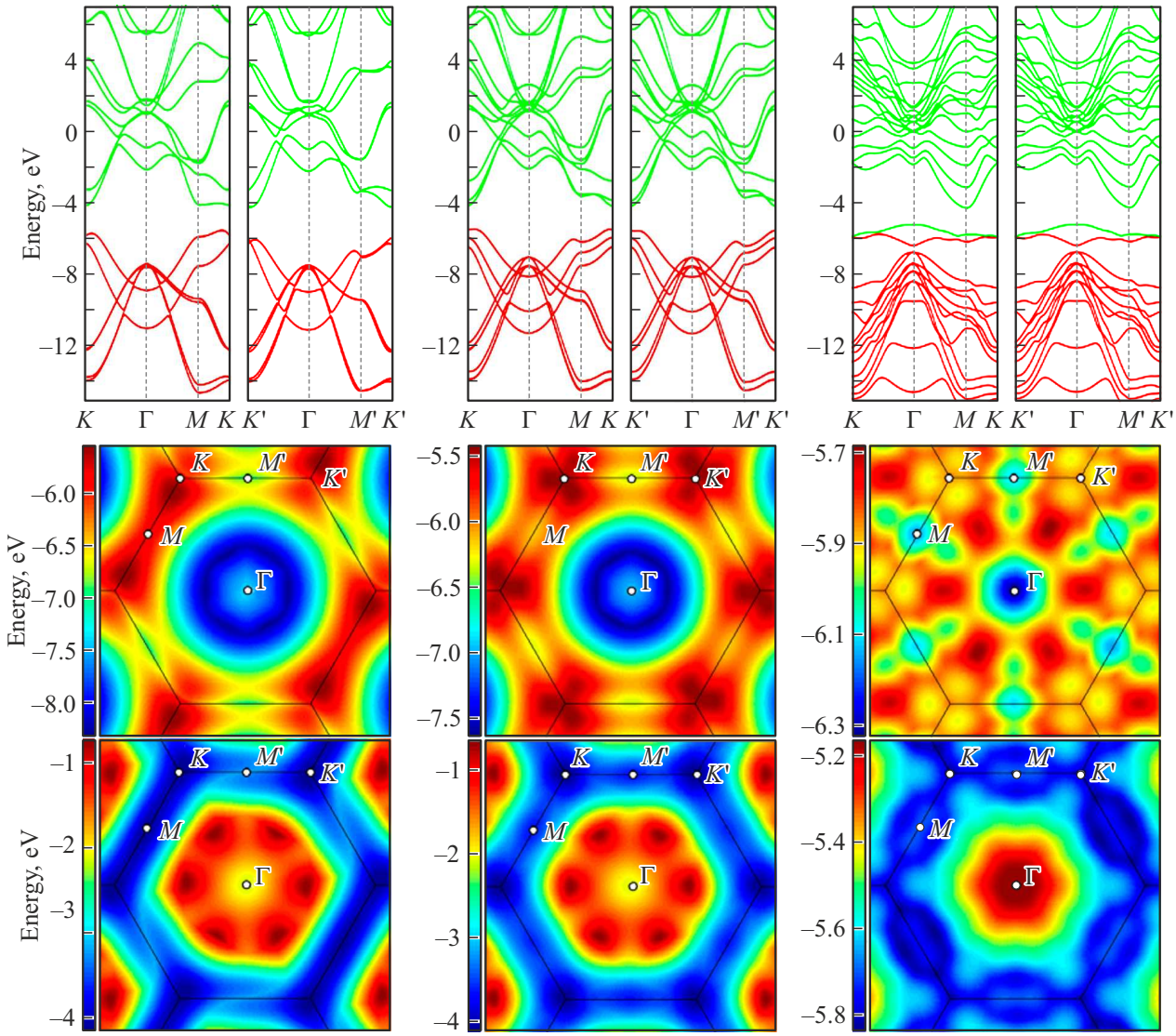

Figure 4. From left to right: data for structures *AB*, *ABA*, *ABAB*. Upper row — band structures, middle row — energy distribution of the HO-orbital, lower row — energy distribution of the LU-orbital.

table). This value is on average 0.5 Å less than the values that were obtained in similar studies [21,24–26].

Diagrams of two-layer and three-layer structures have a form similar to a single-layer configuration. There is no shift of the extremes, there was only an increase of the density of states, which caused a decrease of the width of the interband transitions relative to the monolayer (Figure 4). Thus, the structures have a direct band gap character. It should be noted that the optimization of two-layer configuration was the atoms of the upper layer shifted by a small distance relative to the unoptimized structure, reducing the symmetry to the group m (Figure 5). This arrangement led to an asymmetrical overlap of the orbitals of the atoms of both layers. Therefore, the band gap in this allotrope in the directions ΓK and $\Gamma K'$ are very different: $E_{g(i)} = 1.4\,\text{eV}$ and $E'_{g(i)} = 1.71\,\text{eV}$, respectively (see the table).

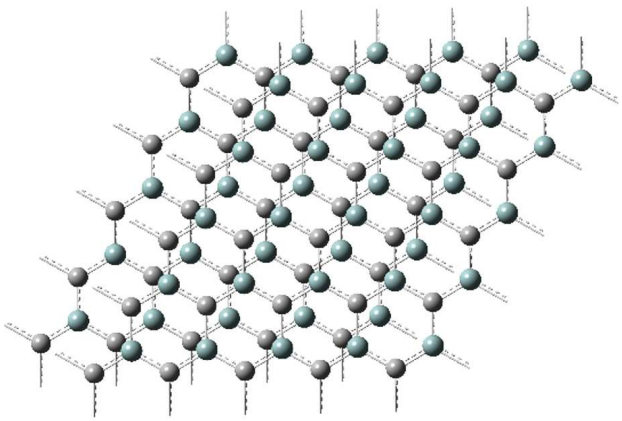

Figure 5. Two-layer structure *AB* before and after optimization.

Structure	R_{Si-C}, Å	R_{sh}, Å	E_b, eV/atom	E_{bsh}, eV/atom	$E_{g(i)}$, eV	$E'_{g(i)}$, eV	$E_{g(d)}$, eV	$E'_{g(d)}$, eV
$A\_$	1.805	–	8.322	–	2	2	2	2
$A\bar{A}$	1.846	2.200	8.444	0.242	2.15	2.15	3.08	3.08
$A\bar{A}\_$	1.837	2.334	8.524	0.403	1.57	1.582	2.176	2.188
$A\bar{A}A\bar{}$	1.843	2.362	8.558	0.463	0.82	0.838	1.996	2
AB	1.805	3.243	8.401	0.156	1.403	1.715	1.483	1.725
ABA	1.804	3.174	8.433	0.223	1.326	1.364	1.346	1.364
$ABAB$	1.89	3.106	8.473	0.293	0.04	0.04	0.04	0.04

The packing symmetry is restored with a further increase of the number of layers of the structure, the three-layer structure has a symmetry group $\bar{6}m2$. The tendency for decrease of the band gap with an increase of the number of layers also persists. A direct transition $E'_{g(d)} = 1.364$ eV was formed in the direction $\Gamma M' K'$ (see the table). The values of the band gap were $E_{g(i)} = 1.326$ eV and $E_{g(d)} = 1.346$ eV for indirect and direct transitions, respectively, in the GMK direction (see the table). The ceiling of the valence band has shifted from the point K towards the point Γ. The difference between direct and indirect transitions is only about 0.02 eV, which indicates a high sensitivity of the properties of this structure to external influences such as temperature or pressure. In particular, it was shown in [27] that in a material with a similar difference between the widths of direct and indirect transitions, direct band gap transitions prevail at temperatures from 300 K and above. Therefore, this structure has prospects for use in optoelectronic devices. The wavelengths corresponding to the interband transitions of the structures are within 723−935 nm, which covers the visible red and near-infrared parts of the spectrum. A more in-depth analysis of structures with this layer packing is required to quantify the impact of external factors on the displacement of the valence band ceiling.

We also present a comparison of the results obtained with data from other studies. The authors of Refs. [21,25,28] demonstrated the indirect nature of these structures. The widths of the band gaps showed a weak dependence on the number of layers. On the contrary, the structures in Ref. [24], have a straight-band character, and an increase of the number of layers leads to a decrease of the band gap. In addition, this work emphasizes that in this package, the band structures in individual sections of the k-space are almost zero-dispersion. Such a property would open up the possibility for designing devices with unique characteristics, for example, with anomalous magnetic properties [29]. Our calculations do not support this conclusion. The graphs in Figure 4 show that the HOMO and LUMO orbitals actually have a lower dispersion in the directions $M-K$ and $M'-K'$. Nevertheless, it is impossible to speak about the completely dispersion-free nature of these sites. Therefore, it is not necessary to expect the manifestation of unusual properties.

The four-layered structure of this family is of particular interest. The quasicrystal cell became similar to the cubic polytype $3C$, the symmetry group was replaced by $3m$. It follows from the analysis of topology and electrophysical properties that the transformation of the initial topology led to the formation of a quasi-crystal formed from graphene and silicene sublattices. The orbitals of neighboring atoms changed the type of hybridization to sp^3, and the original planarity of the layers was disrupted. Nevertheless, the considered structure has a significant difference in the band gap width. Silicon carbide of modification $3C$ has an interband transition of about 2.4 eV [30]. An asymptotic tendency of the width of the interband transition to zero has been established in the four-layer structure. The difference is significant even considering the underestimation of the band gap by the LSDA approximation. There are no similar results in the literature (see, for example, [24,25,28]), which makes this conclusion particularly noteworthy. It can be assumed that the structure became a gapless as a result of the overlap of the electron spectra of graphene and silicene in the sublattice. More precise conclusions can be drawn in a separate study.

4. Conclusion

The band structures of two families of multilayer materials based on monolayers of silicon carbide is studied in the LSDA approximation in this paper. The study of structural changes found that the number of layers and their mutual arrangement make it possible to change the position of the extremes of the valence and conduction bands, as well as to control the band gap. It is shown that the structures of the family $A\bar{A}$ are indirect band gap semiconductors. Packing structures of type AB demonstrate a direct band gap character. At the same time, external conditions, such as temperature, will have a strong impact on their properties. It is established that an increase of the number of layers in both families leads to a decrease of the band gap. By modifying these parameters, it is possible to achieve the formation of devices based on two-dimensional silicon carbide with a wide range of applications with specified characteristics. The discrete series of band gap widths ranges from 0.82 to 2.15 eV covering the spectral range from visible red to near infrared. It has also been found that the band gap sharply decreases in structures of the type AB with a number of layers equal to four, which is a consequence

of the transformation of the structure to a quasi-crystalline one. This makes it possible to further expand the scope of application of multilayer silicon carbide structures.

Funding

The study was supported by Voronezh State University.

Conflict of interest

The authors declare that they have no conflict of interest.

References

[1] A.K. Geim, I.V. Grigorieva. Nature **499**, *7459*, 419 (2013).
[2] A. Rubio, J.L. Corkill, M.L. Cohen. Phys. Rev. B **49**, 5081 (1994).
[3] X. Zhang, L. Jin, X. Dai, G. Chen, G. Liu. ACS Appl. Mater. Interfaces **10**, *45*, 38978 (2018).
[4] D. Chodvadiya, U. Jha, P. Spiewak, K.J. Kurzydłowski, P.K. Jha. Appl. Surf. Sci. **593**, 153424 (2022).
[5] Z. Shi, Zhimingand Zhang, A. Kutana, B.I. Yakobson. ACS Nano **9**, *10*, 9802 (2015).
[6] Q. Wei, Y. Yang, G. Yang, X. Peng. J. Alloys Compd. **868**, 159201 (2021).
[7] A. Kalashnikov, A. Tuchin, L. Bitutskaya. Pisma o materialakh **9**, *2*, 173 (2019). (in Russian).
[8] A.V. Kalashnikov, A.V. Tuchin, L.A. Bityutskaya, T.V. Kulikova. J. Phys. Conf. Ser. **1199**, *1*, 012009 (2019).
[9] T.H. Osborn, A.A. Farajian. J. Phys. Chem. C **116**, *43*, 22916 (2012).
[10] I.J. Wu, G.Y. Guo. Phys. Rev. B **76**, 035343 (2007).
[11] S. Chabi, K. Kadel. Nanomaterials **10**, *11*, (2020).
[12] H.C. Hsueh, G.Y. Guo, S.G. Louie. Phys. Rev. B **84**, 085404 (2011).
[13] X. Chen, J. Jiang, Q. Liang, R. Meng, C. Tan, Q. Yang, S. Zhang, H. Zeng. J. Mater. Chem. C **4**, 7406 (2016).
[14] X. Lin, S. Lin, Y. Xu, A.A. Hakro, T. Hasan, B. Zhang, B. Yu, J. Luo, E. Li, H. Chen. J. Mater. Chem. C **1**, 2131 (2013).
[15] R. Gutzler, J. Schon. Z. Anorg. Allg. Chem. **643**, *21*, 1368 (2017).
[16] H. Sahin, S. Cahangirov, M. Topsakal, E. Bekaroglu, E. Akturk, R.T. Senger, S. Ciraci. Phys. Rev. B **80**, 155453 (2009).
[17] M. Zhao, R. Zhang. Phys. Rev. B **89**, 195427 (2014).
[18] J. Heyd, J. Peralta, G. Scuseria, R. Martin. J. Chem. Phys. **123**, 174101 (2005).
[19] J. O'Connor, J. Smiltens. Silicon Carbide, a High Temperature Semiconductor: Proceedings of the Conference on Silicon Carbide, Boston, Massachusetts, April 2–3, 1959 (Pergamon Press, 1960).
[20] M. Huda, Y. Yan, M. Al-Jassim. Chem. Phys. Lett. **479**, 255 (2009).
[21] Y.-Z. Lan. Comput. Mater. Sci. **151**, 231 (2018).
[22] V. Susi, Tomaand Skakalova, A. Mittelberger, P. Kotrusz, M. Hulman, T.J. Pennycook, C. Mangler, J. Kotakoski, J.C. Meyer. Sci. Rep. **7**, *1*, 4399 (2017).
[23] J. Guan, D. Liu, Z. Zhu, D. Tomanek. Nano Lett. **16**, *5*, 3247 (2016).
[24] A. Yaghoubi, K. Masenelli-Varlot, O. Boisron, S. Ramesh, P. Melinon. Chem. Mater. **30**, *20*, 7234 (2018).
[25] Z. Xu, Y. Li, Z. Liu, C. Li. Phys. E: Low-Dimens. Syst. Nanostructures **79**, 198 (2016).
[26] G. Gao, N.W. Ashcroft, R. Hoffmann. J. Am. Chem. Soc. **135**, *31*, 11651 (2013).
[27] W. Du, S.A. Ghetmiri, B.R. Conley, A. Mosleh, A. Nazzal, R.A. Soref, G. Sun, J. Tolle, J. Margetis, H.A. Naseem, S.-Q. Yu. Appl. Phys. Lett. **105**, *5*, 051104 (2014).
[28] Zh. Xu, Ya. Li, Zh. Liu. Mater. Des. **108**, 333 (2016).
[29] Z. Liu, F. Liu, Y.-S. Wu. Chin. Phys. B **23**, *7*, 077308 (2014).
[30] D. Bimberg, M. Altarelli, N. Lipari. Solid State Commun. **40**, *4*, 437 (1981).

Translated by A.Akhtyamov